Journal of Alloys and Compounds 509 (2011) 6787–6793

Contents lists available at ScienceDirect

Journal of Alloys and Compounds

journal homepage: www.elsevier.com/locate/jallcom

Phase relationships of the Pr–Co–Fe system at 773 K

Wanlin Wang[a,b], Meiwen Lu[a,b], Qiang Feng[a,b], Zhongping Xu[a,b], Lingmin Zeng[a,b,*], Wei He[a,b]

[a] Key Laboratory of New Processing Technology for Nonferrous Metal and Materials, Ministry of Education, Guangxi University, Nanning 530004, China
[b] College of Materials Science and Engineering, Guangxi University, Nanning, Guangxi 530004, China

ARTICLE INFO

Article history:
Received 4 April 2010
Received in revised form 1 April 2011
Accepted 1 April 2011
Available online 8 April 2011

Keywords:
Phase diagram
X-ray diffraction
Scanning electron microscopy

ABSTRACT

The Phase equilibrium of the ternary Pr–Co–Fe system at 773 K was investigated by means of X-ray powder diffraction (XRD), Rietveld method and scanning electron microscopy equipped with energy dispersive X-ray spectroscopy. Nine binary compounds, i.e., Pr_2Co_{17}, $PrCo_5$, Pr_2Co_7, $PrCo_3$, $PrCo_2$, Pr_4Co_3, Pr_5Co_2, Pr_3Co and Pr_2Fe_{17} was confirmed to exist, The maximum solubility of Fe in binary compounds Pr_2Co_{17}, $PrCo_5$, Pr_2Co_7, $PrCo_3$, $PrCo_2$, Pr_4Co_3 and Pr_3Co was determined to be 76.3, 14.1, 15.5, 20.7, 37.5, 2.3 and 2.9 at.%, respectively. No ternary compound was found.

1. Introduction

Rare-earth–transition-metal (RE–TM) intermetallic compounds have been extensively studied in the last decades [1]. Some of these compounds (particularly the cobalt-based ones) show outstanding magnetic properties which make them good materials for the production of permanent magnets [2]. The phase diagram is an important basis for materials research and materials application. For the R–Co–Fe systems, the phase relations have not been investigated systematically until now except the Y–Fe–Co [3], Sm–Fe–Co [4], Gd–Fe–Co [5] and Ho–Co–Fe [6] ternary system. The purpose of the present paper is to provide the phase relationship in the Pr–Co–Fe ternary system at 773 K.

The binary phase diagrams of the Pr–Co, Pr–Fe and Co–Fe systems have been investigated previously and summarized in [7–10]. At 773 K, there is no binary compound in the Co–Fe system. Nine intermetallic compounds Pr_2Co_{17} [11], $PrCo_5$ [12], Pr_5Co_{19} [13], Pr_2Co_7 [14,15], $PrCo_3$ [16], $PrCo_2$ [17], Pr_4Co_3 [18], Pr_5Co_2, [19] and Pr_3Co [14] were found in the Pr–Co system and one intermetallic phase Pr_2Fe_{17} [20,21] in the Pr–Fe system. Shimotamai et al. [22] reported the cubic (C15) laves phase $PrFe_2$ with Cu_2Mg type structure (space group $Fd\bar{3}m$, a = 7.465 Å). But Cannon et al. [23] reported that the $PrFe_2$ phase was synthesized only under high pressures. Buschow [24] investigated the influence of various impurities on the metastable character of the RCo_5 compounds. Binary phase Pr_5Co_{19} was reported by Ray et al. [13] and Wu et al. [8]. According to Okamoto [9], Pr_5Co_{19} was assumed to be a high temperature phase such as the analogous compound Sm_5Co_{19}.

2. Experimental details

The purity of Fe, Co and Pr used in this work is 99.5, 99.8, and 99.5 wt.%, respectively. The 120 samples (Table 1), each weighing 2 g, were prepared by arc melting in a water-cooled copper crucible with a non-consumable tungsten electrode under high pure argon atmosphere. The alloys were re-melted three times in order to achieve complete fusion and homogeneous composition. The weight loss of the alloy samples using in this work was less than 0.6%. After melting, all alloy samples were subjected to a homogenizing anneal in evacuated quartz. The homogenization temperatures of the binary and ternary samples were chosen according to the phase diagrams of the Fe–Pr, Co–Pr and Fe–Co systems. The Co-rich alloys samples were homogenized at 1073 K for 20 days, the Fe-rich alloys samples were homogenized at 873 K for 20 days, the Pr-rich alloys samples were homogenized at 773 K for 20 days. Subsequently, they were cooled to 773 K at a rate of 10 K/h and kept at this temperature for 10 days, then quenched in liquid nitrogen. Most samples were cut in two. One is for X-ray powder diffraction (XRD), the other for metallographic investigation. Samples for X-ray diffraction analyses were powdered. The X-ray powder diffraction measurements were performed on a Rigaku D/max 2500V diffractometer with CuK α radiation and graphite monochromator operated at 40 kV, 250 mA. X-ray powder diffraction patterns of same samples used for Rietveld refinement were collected with a step size of 0.02° and a counting time of 2 s per step.

The Materials Data Inc. software Jade 5.0 [25] and Powder Diffraction File (PDF −4+ 2009) were used for phase identification. The metallographic alloy samples were examined by optical microscopy (DMM660, Caikon, China) and then analyzed by SEM (S-3400N, Hitachi, Japan)/EDX (PV8200, Philip, USA) in backscattered electron (BSE) imaging mode for microstructure observation and composition measurement.

3. Results and discussion

3.1. Binary compounds

Table 2 lists the crystallographic data of the binary compounds in the Pr–Co–Fe system at 773 K. No ternary compounds were fond.

* Corresponding author at: Key Laboratory of New Processing Technology for Nonferrous Metal and Materials, Ministry of Education, Guangxi University, Nanning 530004, China. Tel.: +86 771 3272311; fax: +86 771 3233530.
E-mail address: lmzeng@gxu.edu.cn (L. Zeng).

0925-8388/$ – see front matter © 2011 Elsevier B.V. All rights reserved.
doi:10.1016/j.jallcom.2011.04.006

Table 1
The composition and phase composition of some samples of the Pr–Co–Fe ternary system.

No.	Nominal composition (at.%)			Equilibrated phase	No.	Nominal composition			Equilibrated phase
	Fe	Pr	Co			Fe	Pr	Co	
1	0	10.5	89.5	Pr_2Co_{17}	48	22	40	38	$PrCo_{2-x}Fe_x + Pr_3Co_{1-x}Fe_x$
2	0	15.7	84.3	$PrCo_5 + Pr_2Co_{17}$	49	28	40	32	$PrCo_{2-x}Fe_x + Pr_3Co_{1-x}Fe_x$
3	0	16.7	83.3	$PrCo_5$	50	10	50	40	$PrCo_{2-x}Fe_x + Pr_3Co_{1-x}Fe_x$
4	0	20.5	79.5	$PrCo_5 + Pr_2Co_7$	51	16	50	34	$PrCo_{2-x}Fe_x + Pr_3Co_{1-x}Fe_x$
5	0	24	76	$Pr_2Co_7 + PrCo_3$	52	22	50	28	$PrCo_{2-x}Fe_x + Pr_3Co_{1-x}Fe_x$
6	0	30	70	$PrCo_3 + PrCo_2$	53	8	60	32	$PrCo_{2-x}Fe_x + Pr_3Co_{1-x}Fe_x$
7	0	40	60	$PrCo_2 + Pr_4Co_3$	54	14	60	26	$PrCo_{2-x}Fe_x + Pr_3Co_{1-x}Fe_x$
8	0	50	50	$PrCo_2 + Pr_4Co_3$	55	2	73	25	$Pr_5Co_2 + Pr_3Co_{1-x}Fe_x + Pr_4Co_{3-x}Fe_x$
9	0	60	40	$Pr_4Co_3 + Pr_5Co_2$	56	14	16	70	$Pr_2Co_{17-x}Fe_x + Pr_2Co_{7-x}Fe_x + PrCo_{5-x}Fe_x$
10	0	68	32	$Pr_4Co_3 + Pr_5Co_2$	57	27	16	57	$Pr_2Co_{17-x}Fe_x + Pr_2Co_{7-x}Fe_x + PrCo_{3-x}Fe_x$
11	0	73	27	$Pr_5Co_2 + Pr_3Co$	58	24	20	56	$Pr_2Co_{17-x}Fe_x + Pr_2Co_{7-x}Fe_x + PrCo_{3-x}Fe_x$
12	0	80	20	$Pr_3Co + \alpha Pr$	59	18	22	60	$Pr_2Co_{17-x}Fe_x + Pr_2Co_{7-x}Fe_x + PrCo_{3-x}Fe_x$
13	0	86	14	$Pr_3Co + \alpha Pr$	60	32	16	52	$PrCo_{3-x}Fe_x + PrCo_{2-x}Fe_x + Pr_2Co_{17-x}Fe_x$
14	95	5	0	$Pr_2Fe_{17} + \alpha Fe$	61	35	16	49	$PrCo_{3-x}Fe_x + PrCo_{2-x}Fe_x + Pr_2Co_{17-x}Fe_x$
15	89.5	10.5	0	Pr_2Fe_{17}	62	24	24	52	$PrCo_{3-x}Fe_x + PrCo_{2-x}Fe_x + Pr_2Co_{17-x}Fe_x$
16	84	16	0	$\alpha Pr + Pr_2Fe_{17}$	63	30	24	46	$PrCo_{3-x}Fe_x + PrCo_{2-x}Fe_x + Pr_2Co_{17-x}Fe_x$
17	70	30	0	$\alpha Pr + Pr_2Fe_{17}$	64	36	24	40	$PrCo_{3-x}Fe_x + PrCo_{2-x}Fe_x + Pr_2Co_{17-x}Fe_x$
18	66.7	33.3	0	$\alpha Pr + Pr_2Fe_{17}$	65	30	28	42	$PrCo_{3-x}Fe_x + PrCo_{2-x}Fe_x + Pr_2Co_{17-x}Fe_x$
19	50	50	0	$\alpha Pr + Pr_2Fe_{17}$	66	36	28	36	$PrCo_{3-x}Fe_x + PrCo_{2-x}Fe_x + Pr_2Co_{17-x}Fe_x$
20	30	70	0	$\alpha Pr + Pr_2Fe_{17}$	67	40	16	44	$PrCo_{2-x}Fe_x + Pr_2Co_{17-x}Fe_x$
21	1	74	25	$Pr_3Co_{1-x}Fe_x + Pr_5Co_2$	68	48	16	36	$PrCo_{2-x}Fe_x + Pr_2Co_{17-x}Fe_x$
22	1	80	19	$Pr_3Co_{1-x}Fe_x + \alpha Pr$	69	54	16	30	$PrCo_{2-x}Fe_x + Pr_2Co_{17-x}Fe_x$
23	2	20	78	$Pr_2Co_{7-x}Fe_x + PrCo_{5-x}Fe_x$	70	64	16	20	$PrCo_{2-x}Fe_x + Pr_2Co_{17-x}Fe_x$
24	10	20	70	$Pr_2Co_{7-x}Fe_x + PrCo_{5-x}Fe_x$	71	40	22	38	$PrCo_{2-x}Fe_x + Pr_2Co_{17-x}Fe_x$
25	5	33.3	61.7	$PrCo_{2-x}Fe_x$	72	48	22	30	$PrCo_{2-x}Fe_x + Pr_2Co_{17-x}Fe_x$
26	30	33.3	36.7	$PrCo_{2-x}Fe_x$	73	50	25	25	$PrCo_{2-x}Fe_x + Pr_2Co_{17-x}Fe_x$
27	6	24	70	$Pr_2Co_{7-x}Fe_x + PrCo_{3-x}Fe_x$	74	42	28	30	$PrCo_{2-x}Fe_x + Pr_2Co_{17-x}Fe_x$
28	14	24	62	$Pr_2Co_{7-x}Fe_x + PrCo_{3-x}Fe_x$	75	57	25	18	$PrCo_{2-x}Fe_x + Pr_3Co_{1-x}Fe_x + Pr_2Co_{17-x}Fe_x$
29	8	15	77	$Pr_2Co_{17-x}Fe_x + PrCo_{5-x}Fe_x$	76	40	34	26	$PrCo_{2-x}Fe_x + Pr_3Co_{1-x}Fe_x + Pr_2Co_{17-x}Fe_x$
30	4	12	84	$Pr_2Co_{17-x}Fe_x + PrCo_{5-x}Fe_x$	77	48	34	18	$PrCo_{2-x}Fe_x + Pr_3Co_{1-x}Fe_x + Pr_2Co_{17-x}Fe_x$
31	14	12	74	$Pr_2Co_{17-x}Fe_x + PrCo_{5-x}Fe_x$	78	30	44	26	$PrCo_{2-x}Fe_x + Pr_3Co_{1-x}Fe_x + Pr_2Co_{17-x}Fe_x$
32	4	30	66	$PrCo_{3-x}Fe_x + PrCo_{2-x}Fe_x$	79	36	44	20	$PrCo_{2-x}Fe_x + Pr_3Co_{1-x}Fe_x + Pr_2Co_{17-x}Fe_x$
33	14	29	57	$PrCo_{3-x}Fe_x + PrCo_{2-x}Fe_x$	80	22	54	24	$PrCo_{2-x}Fe_x + Pr_3Co_{1-x}Fe_x + Pr_2Co_{17-x}Fe_x$
34	26	30	44	$PrCo_{3-x}Fe_x + PrCo_{2-x}Fe_x$	81	26	54	20	$PrCo_{2-x}Fe_x + Pr_3Co_{1-x}Fe_x + Pr_2Co_{17-x}Fe_x$
35	8	37	55	$Pr_4Co_{3-x}Fe_x + PrCo_{2-x}Fe_x$	82	14	64	22	$PrCo_{2-x}Fe_x + Pr_3Co_{1-x}Fe_x + Pr_2Co_{17-x}Fe_x$
36	2	48	50	$Pr_4Co_{3-x}Fe_x + PrCo_{2-x}Fe_x$	83	64	25	11	$\alpha Pr + Pr_2Co_{17-x}Fe_x + Pr_3Co_{1-x}Fe_x$
37	4	42	54	$Pr_4Co_{3-x}Fe_x + PrCo_{2-x}Fe_x$	84	49	40	11	$\alpha Pr + Pr_2Co_{17-x}Fe_x + Pr_3Co_{1-x}Fe_x$
38	20	12	68	$Pr_2Co_{17-x}Fe_x + Pr_2Co_{7-x}Fe_x$	85	41	48	11	$\alpha Pr + Pr_2Co_{17-x}Fe_x + Pr_3Co_{1-x}Fe_x$
39	28	12	60	$Pr_2Co_{17-x}Fe_x + Pr_2Co_{7-x}Fe_x$	86	24	60	16	$\alpha Pr + Pr_2Co_{17-x}Fe_x + Pr_3Co_{1-x}Fe_x$
40	18	18	64	$Pr_2Co_{17-x}Fe_x + Pr_2Co_{7-x}Fe_x$	87	30	60	10	$\alpha Pr + Pr_2Co_{17-x}Fe_x + Pr_3Co_{1-x}Fe_x$
41	90	6	4	$\alpha Fe + Pr_2Fe_{17} + Pr_2Co_{17-x}Fe_x$	88	10	74	16	$\alpha Pr + Pr_2Co_{17-x}Fe_x + Pr_3Co_{1-x}Fe_x$
42	60	34	6	$\alpha Pr + Pr_2Fe_{17} + Pr_2Co_{17-x}Fe_x$	89	20	74	6	$\alpha Pr + Pr_2Co_{17-x}Fe_x + Pr_3Co_{1-x}Fe_x$
43	46	50	4	$\alpha Pr + Pr_2Fe_{17} + Pr_2Co_{17-x}Fe_x$	90	10	80	10	$\alpha Pr + Pr_2Co_{17-x}Fe_x + Pr_3Co_{1-x}Fe_x$
44	32	66	2	$\alpha Pr + Pr_2Fe_{17} + Pr_2Co_{17-x}Fe_x$	91	8	44	48	$Pr_4Co_{3-x}Fe_x + PrCo_{2-x}Fe_x + Pr_3Co_{1-x}Fe_x$
45	13	5	82	$Pr_2Co_{17-x}Fe_x + \alpha Fe + \alpha Co$	92	6	50	44	$Pr_4Co_{3-x}Fe_x + PrCo_{2-x}Fe_x + Pr_3Co_{1-x}Fe_x$
46	24	16	60	$Pr_2Co_{17-x}Fe_x + Pr_2Co_{7-x}Fe_x$	93	5	57	38	$Pr_4Co_{3-x}Fe_x + PrCo_{2-x}Fe_x + Pr_3Co_{1-x}Fe_x$
47	14	40	46	$PrCo_{2-x}Fe_x + Pr_3Co_{1-x}Fe_x$	94	3	67	30	$Pr_4Co_{3-x}Fe_x + PrCo_{2-x}Fe_x + Pr_3Co_{1-x}Fe_x$

Table 2
Crystallographic data of the compounds in the Pr–Co–Fe ternary system at 773 K.

Compound	S.G. or symmetry	Structure type	Lattice parameters (Å)			Ref.
			a	*b*	*c*	
α-Fe	$Im\bar{3}m$ (229)	W	2.861			[26]
α-Co	$Fm\bar{3}m$ (225)	Cu	3.544			[27]
α-Pr	$P6_3/mmc$ (194)	La	3.670		11.828	[28]
Pr_2Co_{17}	$R\bar{3}m$ (166)	Th_2Zn_{17}	8.425		12.269	[11]
$PrCo_5$	$P6/mmm$ (191)	$CaCu_5$	5.013		3.980	[12]
Pr_2Co_7	$R\bar{3}m$ (166)	Co_7Er_2	5.06		36.520	[14]
$PrCo_3$	$R\bar{3}m$ (166)	Be_3Nb	5.068		24.79	[16]
$PrCo_2$	$Fd\bar{3}m$ (227)	Cu_2Mg	7.312			[17]
Pr_4Co_3	$P\bar{6}$ (174)	Cu_3La_4	5.880		9.649	[18]
Pr_5Co_2	$C2/c$ (15)	B_2Pd_5	16.54	6.48	7.10	[19]
Pr_3Co	$Pnma$ (62)	CFe_3	7.143	9.780	6.410	[14]
Pr_2Fe_{17}	$R\bar{3}m$ (166)	Th_2Zn_{17}	8.585		12.464	[21]

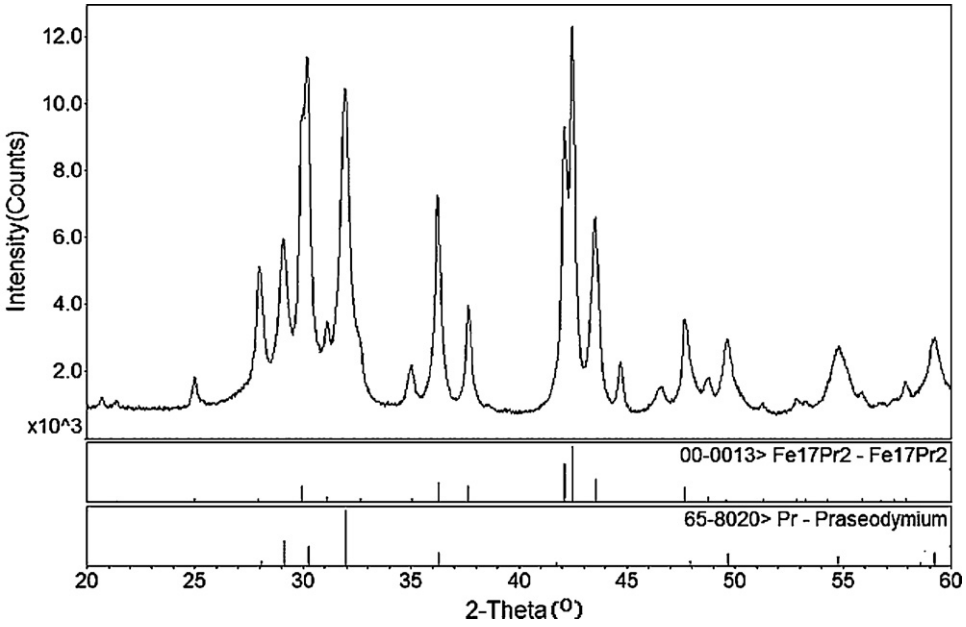

Fig. 1. XRD patterns of the sample No. 18 ($Pr_{33.3}Fe_{66.7}$) contained the phases of Pr_2Fe_{17} and α-Pr.

Nine intermetallic phases, i.e., Pr_2Co_{17}, $PrCo_5$, Pr_2Co_7, $PrCo_3$, $PrCo_2$, Pr_4Co_3, Pr_5Co_2, Pr_3Co and Pr_2Fe_{17} accept for Pr_5Co_{19} and Pr Fe_2 have been confirmed to exist in our work. In order to identify the presence or absence of the phase Pr Fe_2, an alloy sample (No. 18) with composition of $Pr_{33.33}Fe_{66.67}$ was prepared. Fig. 1 shows the X-ray diffraction patterns of this alloy sample. From Fig. 1, it can be seen that the sample No. 18 consists of the two phases of Pr_2Fe_{17} and α-Pr. No evidence was found to confirm the existence of Pr Fe_2 under our experimental conditions. Mansey et al. [29] indicated that In the system "$PrFe_2$–$PrCo_2$", the cubic C15 phase based upon $PrCo_2$ is stable at mole fractions exceeding 0.5 of $PrCo_2$, with less than 0.25 mole fraction of $PrCo_2$ no laves phase was detected in the diffraction photographs. Our result about the absence of $PrFe_2$ is in good agreement with the observation by Mansey et al. and as well as the results reported in Refs. [20,23,30,31]. The X-ray diffraction patterns of the sample No. 4 with $Pr_{20.5}Co_{79.5}$ nominal composition are shown in Fig. 2. It is obvious that the sample No. 4 consists of $PrCo_5$ and Pr_2Co_7 phases. In other words the compound Pr_5Co_{19} was not existent. This result agrees well with the results reported in Refs. [32,33].

3.2. Solid solution

In order to determine solid solution of Fe in Pr_2Co_{17} precisely, ten samples with nominal composition of $Pr_2Co_{17-x}Fe_x$ (x = 0, 3.17, 3.80, 5.51, 7.03, 8, 10, 12, 14, 16, 17) were prepared and standard

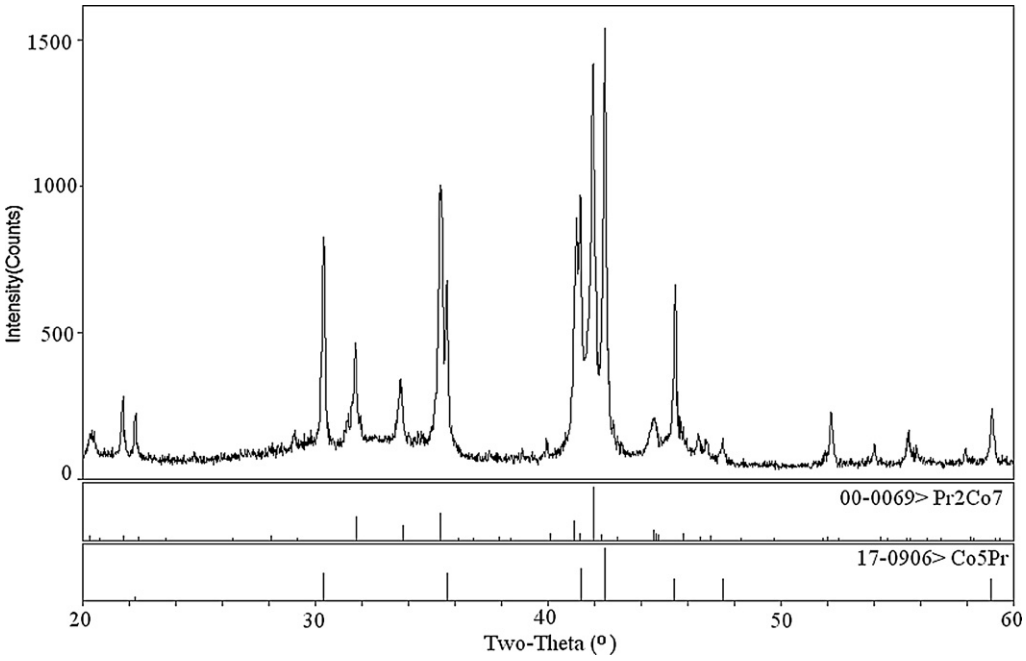

Fig. 2. XRD patterns of the sample No. 4 ($Pr_{20.5}Co_{79.5}$) contained the phases of Pr_2Co_7 and $PrCo_5$.

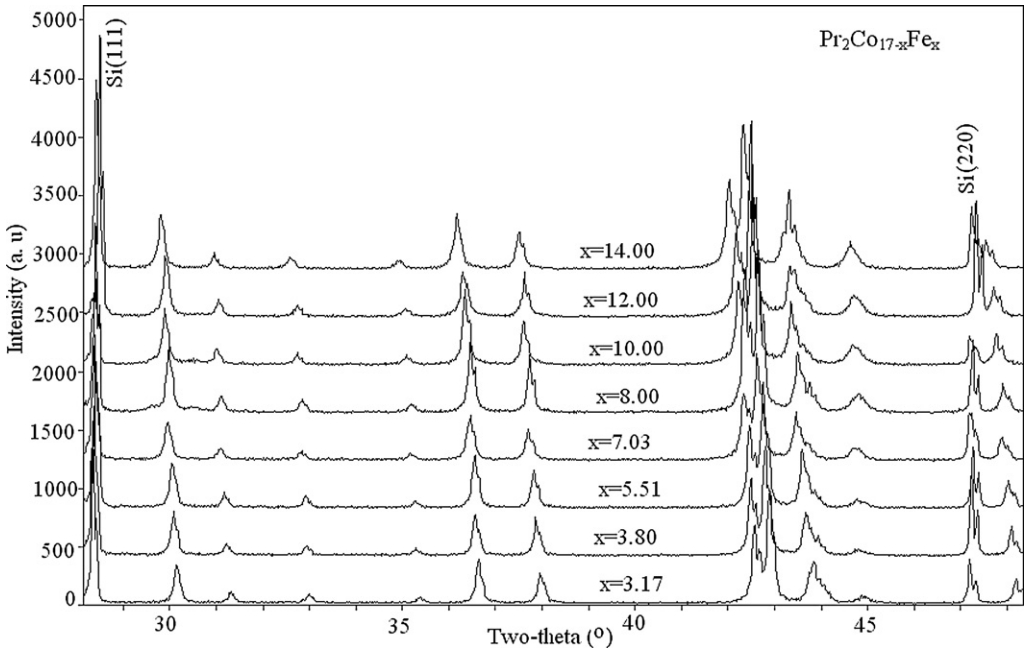

Fig. 3. XRD patterns ($28.2^\circ < 2\theta < 48.2^\circ$) of the $Pr_2Co_{17-x}Fe_x$ alloys with $x = 0$, 3.17, 3.80, 5.51, 7.03, 8, 10, 12, 14.

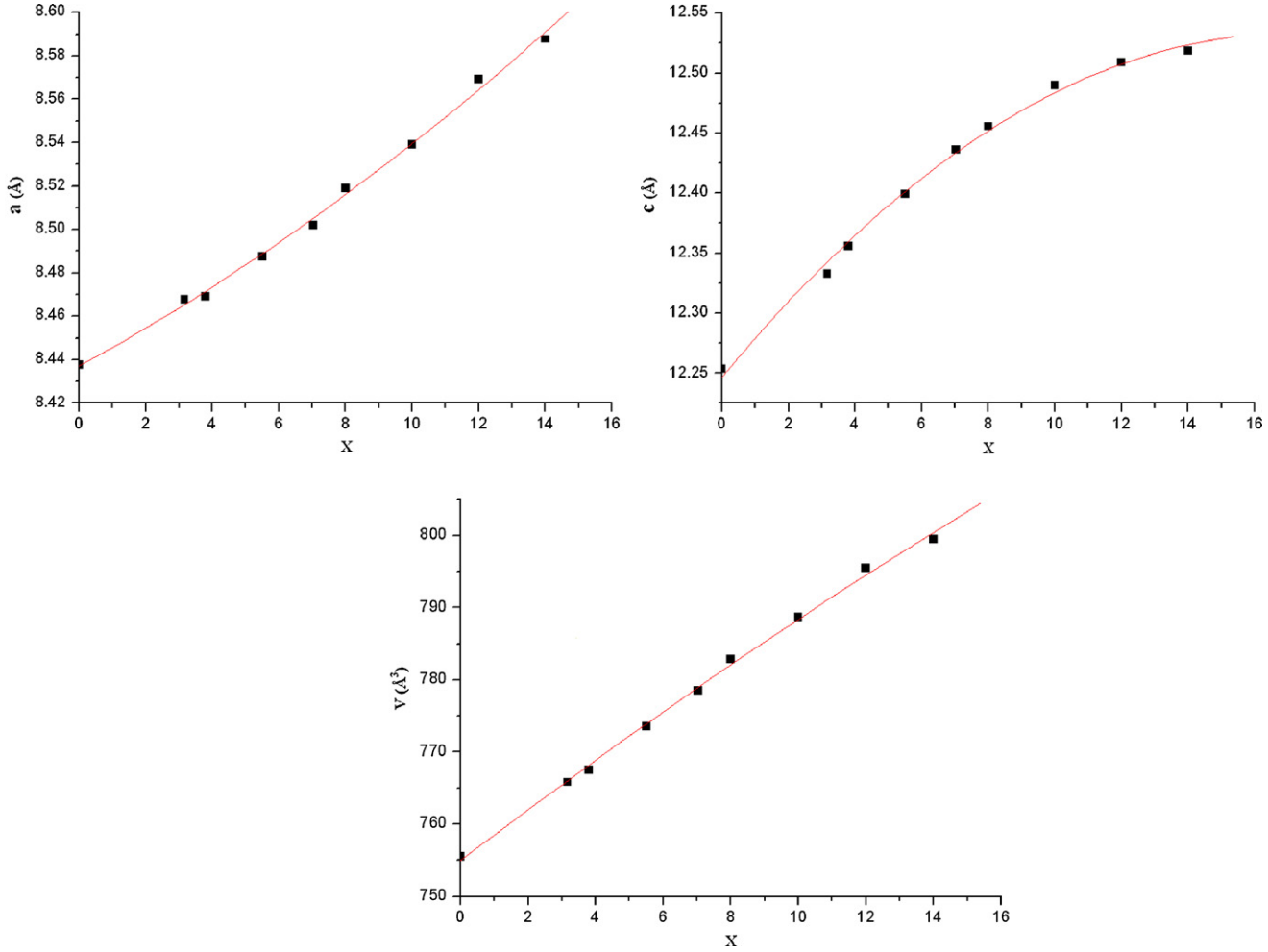

Fig. 4. Variation of Lattice parameters and cell volume as a function of x in $Pr_2Co_{17-x}Fe_x$.

reference material (SRM 640c) was added to each sample. The X-ray diffraction data were collected in the 2θ range from 26° to 90° and calibrated using SRM 640c as an internal reference. Fig. 3 shows the powder X-ray diffraction patterns ($28.2° < 2\theta < 48.2°$) of the $Pr_2Co_{17-x}Fe_x$ alloys with $x = 0$, 3.17, 3.80, 5.51, 7.03, 8, 10, 12, 14. From Fig. 3 we can see that there is no phase change in the XRD patterns except shifts in the positions of Bragg reflections towards lower 2θ angles. Accurate lattice parameters were obtained by a least-squares refinement of the calibrated data. The lattice parameters and cell volume are listed in Table 3 and are plotted as a function of x in Fig. 4(a and b). Because the sample with $x = 16$ is two phases, so we can deduce that the value of x should be greater than 14 and less than 16. Combining the result obtained from the Ritveld refinement of sample No. 75 ($Pr_{25}Co_{18}Fe_{57}$), we obtained the maximum solubility of Fe in Pr_2Co_{17} is about 76.3 at.% at 773 K, it is close to that reported by Satyanarayana et al. [34].

We also observed the formation of solid solution for the $PrCo_5$, Pr_2Co_7, $PrCo_3$, $PrCo_2$, Pr_4Co_3 and $CoPr_3$ compounds. Similarly, the solid solubility of Fe in other binary compounds was determined by lattice parameter method, Rietveld method or by SEM/EDX technique. On the basis of the results of experiment, the maximum solid solubility of Fe in binary compounds $PrCo_5$, Pr_2Co_7, $PrCo_3$, $PrCo_2$, Pr_4Co_3 and Pr_3Co was determined to be 14.1, 15.5, 20.7, 37.5, 2.3 and 2.9 at.%, respectively.

3.3. Isothermal section of the Pr–Co–Fe ternary system at 773 K

Both of SEM/EDX technique and quantitative phase analysis using Rietveld method were used to detect the phase composition of a sample located in the three-phase region. Fig. 5(a) is the SEM image of sample No. 56 ($Pr_{16}Co_{70}Fe_{14}$). It can be observed that there are three different phase. The composition of these three phases analyzed by SEM-EDX with ZAF matrix corrections was $Pr_{11.1}Co_{72.2}Fe_{16.7}$, $Pr_{18.9}Co_{67.1}Fe_{14.0}$, and

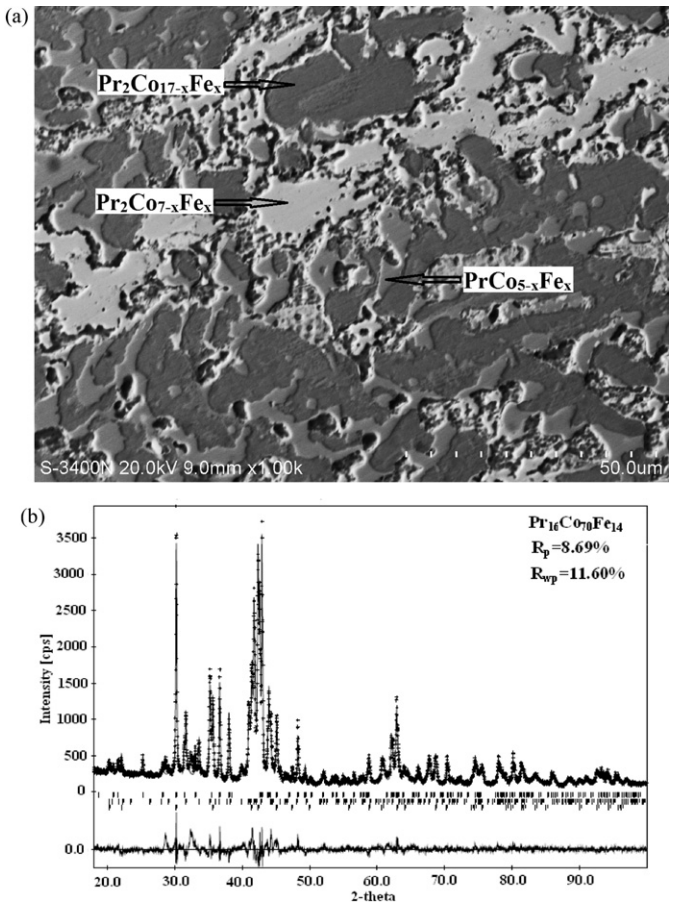

Fig. 5. (a) SEM image of sample No. 56 ($Pr_{16}Fe_{14}Co_{70}$) and (b) Rietveld refinement results for the same sample indicated the existence of the three phase $Pr_2Co_{17-x}Fe_x$ ($x = 3.17$), $PrCo_{5-x}Fe_x$ ($x = 0.91$) and $Pr_2Co_{7-x}Fe_x$ ($x = 1.39$).

Table 3
The lattice parameters and cell volume of the compound $Pr_2Co_{17-x}Fe_x$.

x	Composition of Fe (at.%)	a (Å)	c (Å)	v (Å^3)
0	0	8.4377(2)	12.2539(5)	755.5321
3.17	16.7	8.4678(5)	12.3330(1)	765.8441
3.80	20	8.4691(4)	12.3560(5)	767.5079
5.51	29	8.4876(5)	12.3994(2)	773.5723
7.03	37	8.5019(7)	12.4364(3)	778.4973
8.0	42.1	8.5190(3)	12.4558(6)	782.8513
10.0	52.6	8.5390(4)	12.4899(7)	788.6847
12.0	63.2	8.5691(6)	12.5091(1)	795.4757
14.0	73.7	8.5877(4)	12.5184(5)	799.5260

Table 4
The Rietveld method and SEM/EDX experimental results for some alloys in the Pr–Co–Fe system at 773 K.

No.	Nominal composition (at.%)			Phase composition (at.%)			Phase analysis by Rietveld method	Lattice parameters (Å) obtained by Rietveld method		
	Pr	Co	Fe	Pr	Co	Fe		a	b	c
56	16	70	14	11.1	72.2	16.7	$Pr_2Co_{17-x}Fe_x$ ($x = 3.17$)	8.4678(5)	8.4678(5)	12.3330(1)
				21.9	62.6	15.5	$Pr_2Co_{7-x}Fe_x$ ($x = 1.39$)	5.08611(3)	5.08611(3)	36.7790(4)
				18.9	67.1	14.0	$PrCo_{5-x}Fe_x$ ($x = 0.91$)	5.02757(2)	5.02757(2)	4.01233(2)
60	16	52	32	9.4	53.5	37.1	$Pr_2Co_{17-x}Fe_x$ ($x = 7.03$)	8.5019(7)	8.5019(7)	12.4364(3)
				35.3	28.6	36.1	$PrCo_{2-x}Fe_x$ ($x = 1.11$)	7.4298(4)	7.4298(4)	7.4298(4)
				27.8	51.5	20.7	$PrCo_{3-x}Fe_x$ ($x = 0.87$)	5.1147(1)	5.1147(1)	24.8072(9)
75	25	18	57	12.1	12.4	75.5	$Pr_2Co_{17-x}Fe_x$ ($x = 14.5$)	8.5883(4)	8.5883(4)	12.5196(7)
				32.9	29.6	37.5	$PrCo_{2-x}Fe_x$ ($x = 1.2$)	7.4302(2)	7.4302(2)	7.4302(2)
				72.3	23.9	3.8	$Pr_3Co_{1-x}Fe_x$ ($x = 0.11$)	7.1351(8)	9.8162(10)	6.4327(8)
93	57	38	5	33.2	54.9	11.9	$PrCo_{2-x}Fe_x$ ($x = 0.35$)	7.4215(5)	7.4215(5)	7.4215(5)
				74.7	22.4	2.9	$Pr_3Co_{1-x}Fe_x$ ($x = 0.12$)	7.1359(1)	9.8178(2)	6.4304(1)
				55.8	41.9	2.3	$Pr_4Co_{3-x}Fe_x$ ($x = 0.16$)	5.863(2)	5.863(2)	9.617(2)

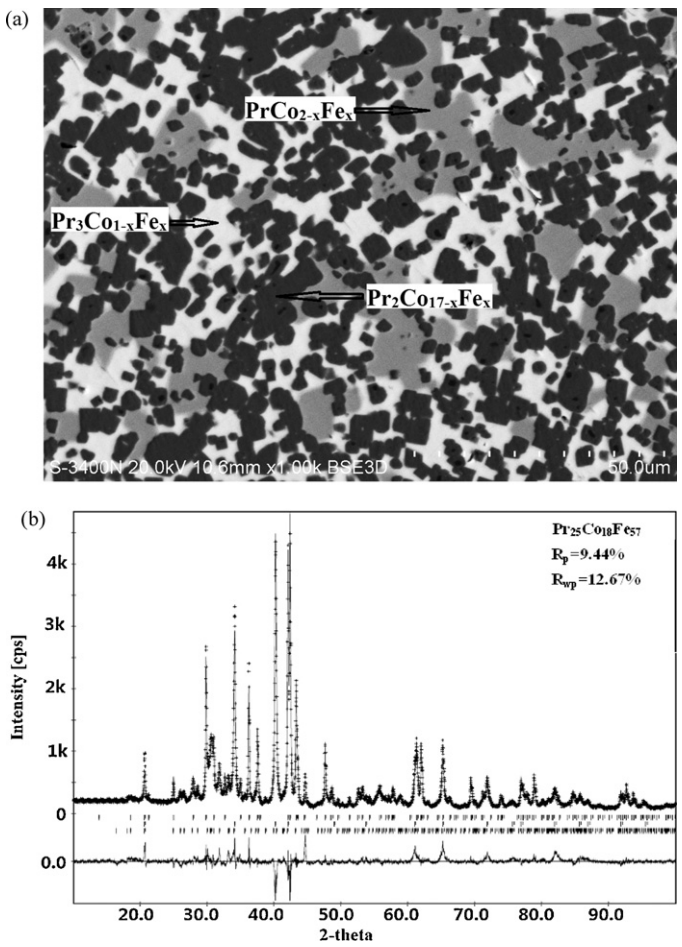

Fig. 6. (a) SEM image of sample No. 75 ($Pr_{25}Co_{18}Fe_{57}$) and (b) Rietveld refinement results for the same sample indicated the existence of the three phase $Pr_2Co_{17-x}Fe_x$ ($x = 14.5$), $PrCo_{2-x}Fe_x$ ($x = 1.2$) and $Pr_3Co_{1-x}Fe_x$ ($x = 0.11$).

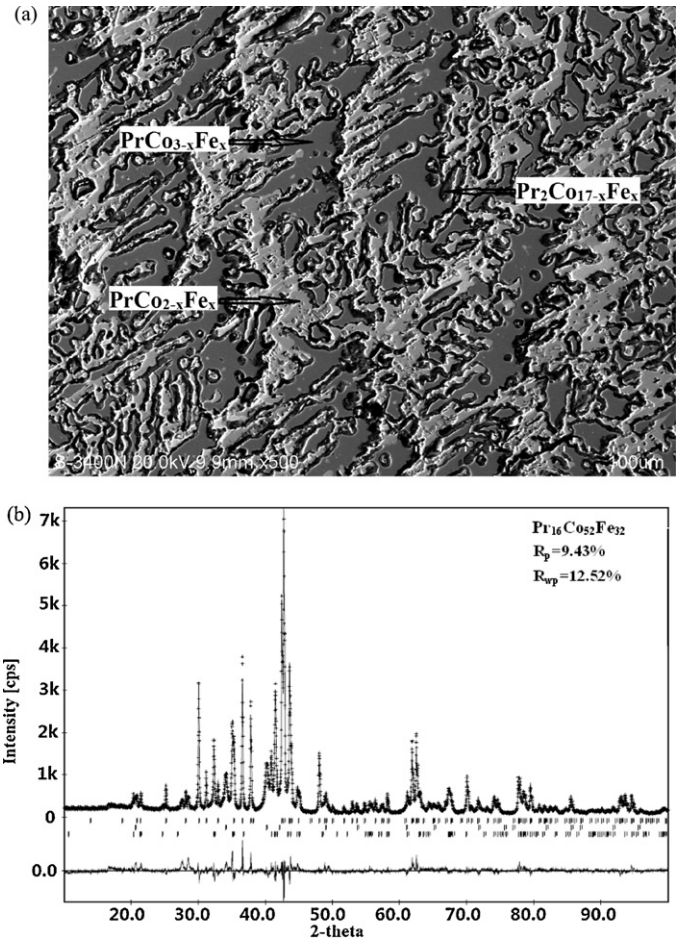

Fig. 7. (a) SEM image of sample No. 60 ($Pr_{16}Co_{52}Fe_{32}$) and (b) Rietveld refinement results for the same sample indicated the existence of the three phase $Pr_2Co_{17-x}Fe_x$ ($x = 7.09$), $PrCo_{3-x}Fe_x$ ($x = 0.87$) and $PrCo_{2-x}Fe_x$ ($x = 1.11$).

$Pr_{21.9}Co_{62.6}Fe_{15.5}$, respectively. Fig. 5(b) is the quantitative phase analysis results using Rietveld method for the same sample No. 56 ($Pr_{16}Co_{70}Fe_{14}$). It also contains three phases of $Pr_2Co_{17-x}Fe_x$, $PrCo_{5-x}Fe_x$ and $Pr_2Co_{7-x}Fe_x$. Rietveld refinement shows when Fe atoms randomly distribute on Co sites of Pr_2Co_{17}, $PrCo_5$ and Pr_2Co_7 with 0.19, 0.18 and 0.20 occupation fraction respectively, i.e., the composition of these three phases is $Pr_{10.53}Co_{72.47}Fe_{17}$, $Pr_{16.67}Co_{68.33}Fe_{15}$ and $Pr_{22.22}Co_{62.22}Fe_{15.56}$ respectively, the refinement results are the best ($R_p = 8.69\%$, $R_{wp} = 11.60\%$). It can be seen that the results obtained from Rietveld refinement are in good agreement with that determined by SEM-EDX. The Rietveld refinement and the SEM image for some representative samples No. 56 ($Pr_{16}Co_{70}Fe_{14}$), No. 75 ($Pr_{25}Co_{18}Fe_{57}$), No. 60 ($Pr_{16}Co_{52}Fe_{32}$) and No. 55 ($Pr_{73}Co_{25}Fe_2$) located in corresponding three phase regions are shown in Figs. 6–8. Table 4 lists the nominal compositions of No. 56, No. 60, No. 75 and No. 93 alloy samples, the phase composition determined by SEM/EDX, the phase content and the lattice parameters obtained by Rietveld refinement method.

On the basis of the results of XRD and SEM/EDX analysis, nine binary phases, i.e., Pr_2Co_{17}, $PrCo_5$, Pr_2Co_7, $PrCo_3$, $PrCo_2$, Pr_4Co_3, Pr_5Co_2, Pr_3Co and Pr_2Fe_{17} have been confirmed to exist, ten three-phase regions were observed in the present work. They are: $Pr_2Co_{17-x}Fe_x + \alpha Fe + \alpha Co$; $Pr_2Co_{17-x}Fe_x + Pr_2Co_{7-x}Fe_x + PrCo_{5-x}Fe_x$; $Pr_2Co_{17-x}Fe_x + Pr_2Co_{7-x}Fe_x + PrCo_{3-x}Fe_x$; $PrCo_{2-x}Fe_x + Pr_3Co_{1-x}Fe_x + Pr_2Co_{17-x}Fe_x$; $PrCo_{2-x}Fe_x + Pr_3Co_{1-x}Fe_x + Pr_2Co_{17-x}Fe_x$; $\alpha Pr + Pr_2Co_{17-x}Fe_x + Pr_3Co_{1-x}Fe_x$; $Pr_4Co_{3-x}Fe_x + PrCo_{2-x}Fe_x + Pr_3Co_{1-x}Fe_x$; $Pr_5Co_2 + Pr_3Co_{1-x}Fe_x + Pr_4Co_{3-x}Fe_x$; $\alpha Fe + Pr_2Fe_{17} + Pr_2Co_{17-x}Fe_x$; $\alpha Pr + Pr_2Fe_{17} + Pr_2Co_{17-x}Fe_x$. The isothermal section of the Pr–Co–Fe ternary system at 773 K is constructed and presented in Fig. 9. No ternary compounds were found.

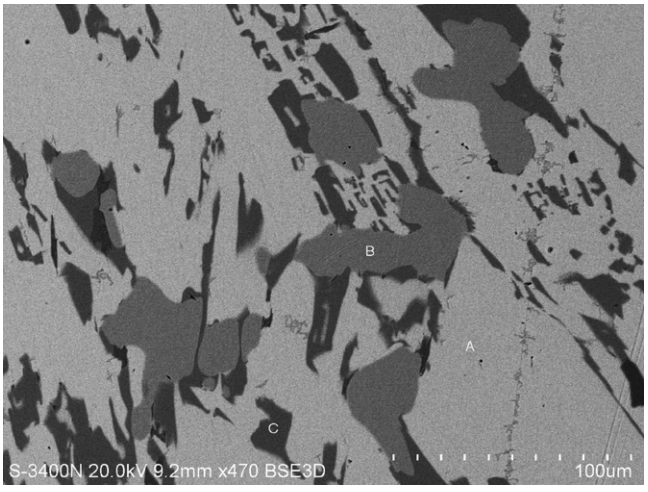

Fig. 8. SEM image of sample No. 55 ($Co_{73}Pr_{73}Fe_2$) indicated the existence of the three phases. A: $Pr_3Co_{1-x}Fe_x$ ($x = 0.11$), B: Pr_5Co_2, and C: $Pr_4Co_{3-x}Fe_x$ ($x = 0.16$).

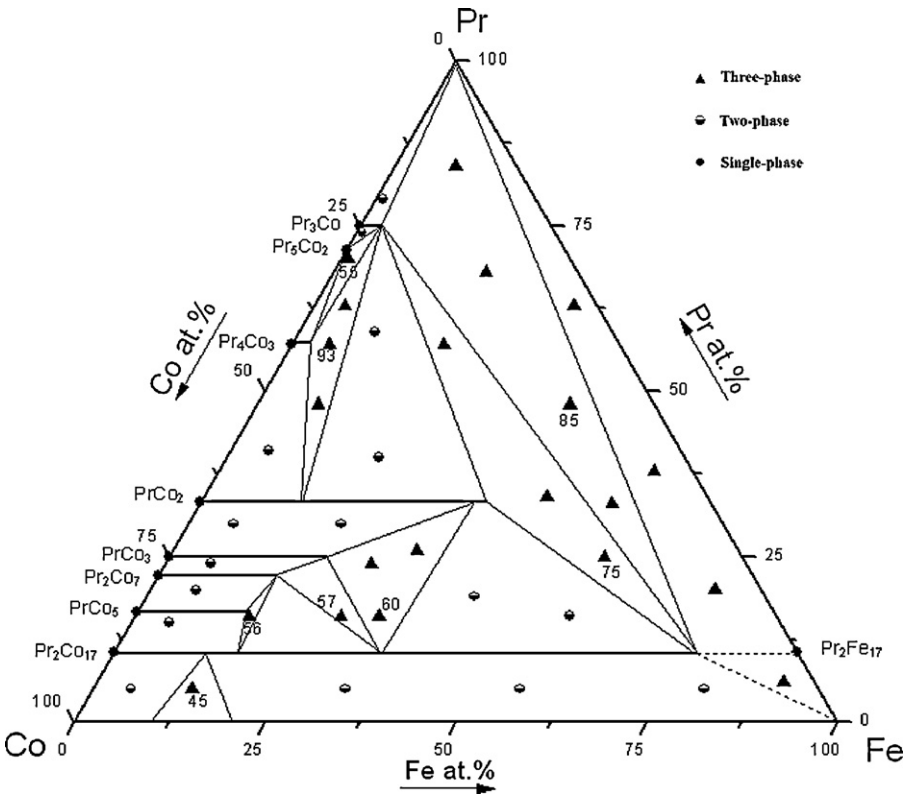

Fig. 9. Isothermal section of the phase diagram of the Pr–Co–Fe ternary system at 773 K.

4. Conclusion

The isothermal section of the Pr–Co–Fe ternary system at 773 K has been determined by using our experimental results obtained by comparison of the X-ray diffraction patterns, SEM/EDX and Rietveld refinement method. There are 9 binary compounds and no ternary compound. The maximum solubility of Fe in binary compounds Pr_2Co_{17}, $PrCo_5$, Pr_2Co_7, $PrCo_3$, $PrCo_2$, Pr_4Co_3 and Pr_3Co was determined to be 76.3, 14.1, 15.5, 20.7, 37.5, 2.3 and 2.9 at.%, respectively.

Acknowledgement

This work was jointly supported by the National Natural Science Foundation of China (Grant No. 50861005).

References

[1] K.H.J. Buschow, Rep. Prog. Phys. 54 (1991) 1123.
[2] L. Pareti, A. Paoluzi, J. Magn. Magn. Mater. 251 (2002) 178–185.
[3] Y.C. Chuang, C.H. Wu, Y.C. Chang, J. Less-Common Met. 118 (1) (1986) 7–20.
[4] G. Schneider, E.-Th. Henig, H.L. Lukas, G. Petzow, J. Less-Common Met. 110 (1985) 159–170.
[5] J. Huang, H. Zhong, X. Xia, W. He, J. Zhu, J. Deng, Y. Zhuang, J. Alloy Compd. 471 (2009) 74–77.
[6] W. He, Y. Zhao, Y. Zhang, M. Yu, L. Zeng, J. Alloy Compd. 509 (2011) 632–635.
[7] A.E. Ray, Cobalt 1 (1974) 3.
[8] C.H. Wu, Y.C. Chuang, X.M. Zin, X.H. Guan, Z. Metallkd. 83 (1992) 32.
[9] H. Okamoto, J. Phase Equilibr. 13 (1992) 675.
[10] T.B. Massalski, H. Okamoto, P.R. Subramanian, L. Kacprzak (Eds.), Binary Alloy Phase Diagrams, vol. 2, 2nd ed., The Materials Information Society, Materials Park, OH, 1990.
[11] H. Oesterreicher, J. Less-Common Met. 32 (1973) 385.
[12] W.A.J.J. Velge, K.H.J. Buschow, J. Appl. Phys. 39 (3) (1968) 1717–1720.
[13] A.F. Ray, A.T. Bierman, R.S. Harmer, J.E. Davison, Cobalt (Engl. Ed.) 4 (1973) 90.
[14] K.H.J. Buschow, Philips Res. Rep. 26 (1971) 49.
[15] Y. Khan, Acta Crystallogr., Sec. B: Struct. Crystallogr. Cryst. Chem. 30 (1974) 1533.
[16] V.V. Burnasheva, V.A. Klimeshin, V.A. Yartys', K.N. Semenenko, Izvestiya Akademii Nauk SSSR, Neorganicheskie Materialy 15 (1979) 801–806.
[17] Schweizer, J. Phys. Lett. A 24 (13) (1967) 739–740.
[18] C.H. Wu, Inst. of Metal Research, Academia Sinica, Shenyang, China, Private Communication, 1993.
[19] J.M. Moreau, D. Paccard, Acta Crystallogr., Sec. B: Struct. Crystallogr. Cryst. Chem. 32 (1976) 1654.
[20] H. Okamoto (Ed.), Phase Diagrams of Binary Iron Alloys, ASM International, Materials Park, OH, 1993, pp. 341–349.
[21] Q. Johnson, D.H. Wood, G.S. Smith, Acta Crystallogr. B 24 (1968) 274–276 (24,1968–38,1982).
[22] M. Shimotamai, H. Fujisawa, M. Doyama, J. Magn. Magn. Mater. 47 (1985) 102–104.
[23] J.F. Cannon, D.L. Robertson, H.T. Hall, Mater. Res. Bull. 7 (1972) 5–12.
[24] K.H.J. Buschow, J. Less-Common Met. 37 (1974) 91–101.
[25] Materials Data JADE Release 5.0, XRD Pattern Processing, Materials Data Inc., Livermore, CA, 2002.
[26] A.J. Bradley, A.H. Jay, J. Iron Steel Inst. Lond. 125 (1932) 339.
[27] E.A. Owen, D. Madoc-Jones, Proc. Phys. Soc. Lond. 67 (1954) 459.
[28] J.J. Hanak, A.H. Daane, J. Less-Common Met. 3 (1961) 110.
[29] R.C. Mansey, G.V. Raynor, I.R. Harris, J. Less-Common Met. 14 (1968) 337–347.
[30] J. Ren, F. Gu, G. Cheng, H. Zhou, J. Alloy Compd. 394 (2005) 211–214.
[31] J. Liu, W. Liu, B. Zong, L. Wang, X. Cui, J. Li, J. Alloy Compd. 456 (2008) 101–104.
[32] S. Baèr, H.-J. Schaller, Thermochim. Acta 314 (1998) 131–136.
[33] Y. Chen, J. Liang, J. Alloy Compd. 289 (1999) 96–98.
[34] M.V. Satyanarayana, H. Fujll, W.E. Wallace, J. Magn. Magn. Mater. 40 (1984) 241–246.